System Efficiency Measurement through Bond Graph Modeling

Robert T. McBride
Raytheon Missile Systems
P.O. Box 11337, Bldg. 805, M/S L-5
Tucson, AZ, 85734-1337, USA
rtmcbride@raytheon.com

François E. Cellier
University of Arizona
P.O. Box 210104,
Tucson, AZ, 85721-0104, USA
cellier@ece.arizona.edu

Keywords: Dymola, Modelica, object-oriented physical system modeling, graphical modeling, efficiency.

Abstract

Bond-graph modeling is a method of modeling a physical system by mapping the power flow through the system. Generally the power flow information of a bond-graph is used to develop the equations of motion for a given system. In this paper, the power flow information of a bond-graph is used in a very different way. This paper presents a method, in which the power flow information is used to monitor the effectiveness of a control scheme. The energy output of a system divided by the energy put into the system gives a feel for the efficiency of the system.

This paper shows, by means of an example, a method in which a bond-graph model can be used to compare a system's response to its thermodynamic theoretical limit. Two separate control schemes are shown and the system responses are compared. A comparison of the effectiveness of two controllers is made by observing their ability to utilize the power supplied by the motor. By monitoring the power flow through the bond-graph, for a given controller, one can get an idea of the controller's ability to effectively use the energy available to the system.

INTRODUCTION

In a given system, limitations exist on the amount of power that the system can use at any given time. These limitations can be used to determine the theoretical limit of the system's response. In the case of a control system, often the performance of the system is limited by the thermodynamic bounds of the actuator. A properly designed controller will make use of the total available energy allowed in the actuator. Since bond-graphs map the power flow through a system, a bond-graph model of an actuator can be used to monitor the actuator's thermodynamic response as compared to its theoretical limit. In this way, one can determine if the control system has been properly designed.

The equations obtained from a bond-graph model are identical to equations obtained through other modeling techniques. However, in this research the power flow map is used specifically to monitor the used energy in the system and compare it to how much energy the system could possibly use. Thus bond-graph modeling lends itself naturally to this analysis.

In this paper, a bond-graph of a servo-positioning system is used to demonstrate the energy based analysis of two separate controller schemes.

THE SERVO-POSITIONING SYSTEM

A controller, motor, and load dynamics are shown in figure 1. This system represents a fin positioning system used in flight control. The command input is a position command in degrees. The fin position is fed back to the controller in radians. The modeling software used to create the models shown is Dymola [1].

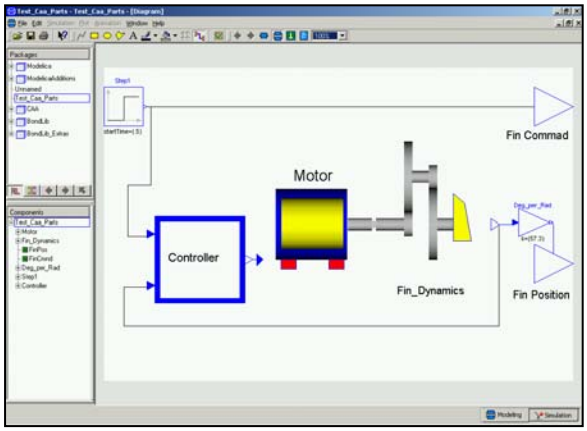

Figure 1. Fin Positioning System

Inside the motor block of figure 1 is a bond-graph model of the motor dynamics. The bond-graph model

was created in Dymola using the Dymola Bond-Graph Library [2]. The motor dynamics consist of three parts; battery dynamics, motor coils, and shaft dynamics. The battery has a protective diode that is modeled as a non-linear resistor. The logic for this resistance is as follows:

if (Voltage of the capacitor *cbatt* > *e0*) then
    mR1 = .1
else
    mR1 = 500
end

Although this detail is not explicitly shown in the bond-graph diagram of figure 2, it is stated in the Dymola description of the model.

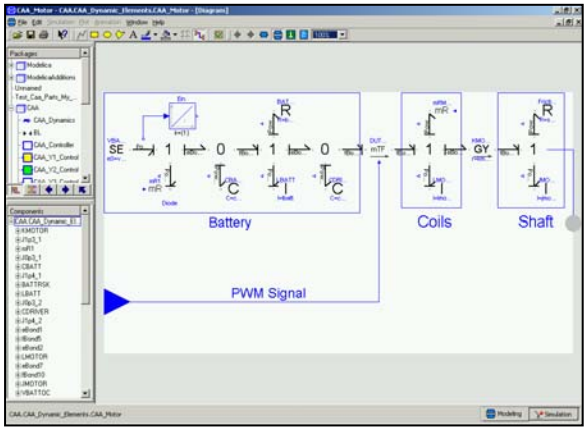

Figure 2. Motor Bond-Graph

In order to make figure 2 more readable, figures 2A and 2B have been included which zoom in on the details of figure 2.

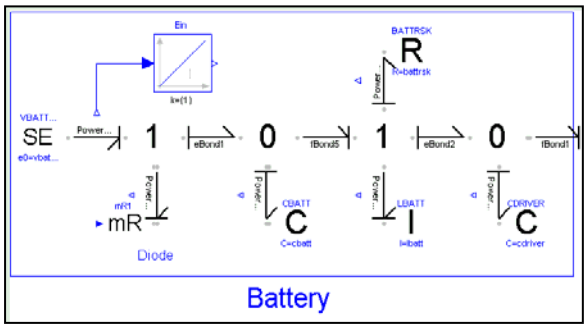

Figure 2A. Motor Bond-Graph: Battery

Shown in figure 2 is a modulated transformer. This element is used to implement the pulse width modulated (PWM) signal. As seen by the motor bond-graph, the PWM signal limits the amount of power flow from the battery to the rest of the servo-system. In this way the fin can be commanded to a specific position.

The signal flow outputs on some of the bonds in figures 2 and 3 allow Dymola, the modeling software, to monitor the power flow in these bonds. This information will later be used to determine the effectiveness of a given controller.

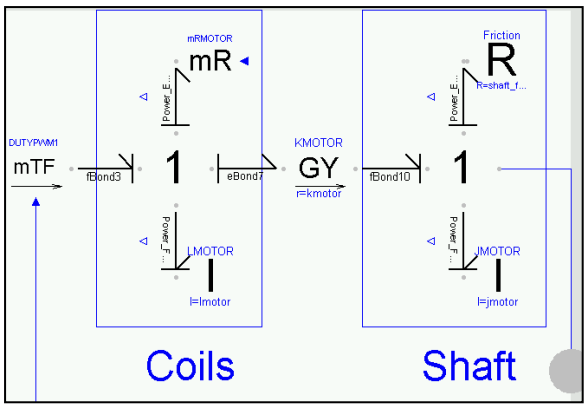

Figure 2B. Motor Bond-Graph: Coil and Shaft

The non-linear resistor shown in figure 2B also acts as a diode. The logic with which this resistance is implemented is as follows:

if (abs(*PWM Signal*) >= .05) then
    mRMOTOR = .63
else
    mRMOTOR = 4.53 – 78*abs(*PWM Signal*)
end

The fin dynamic equations are modeled in the bond-graph of figure 3. The output of the model is the fin position.

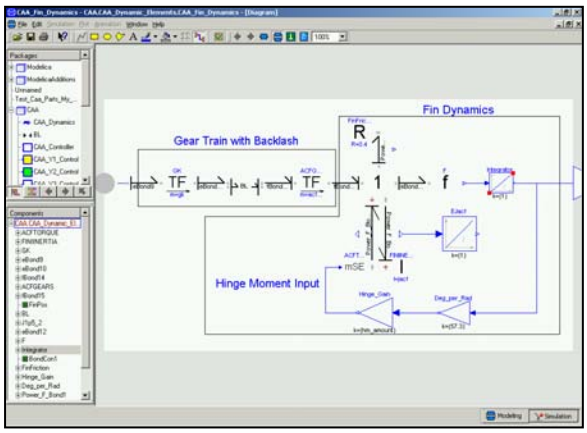

Figure 3. Gear Train and Fin Dynamics

The fin position is calculated by integrating the flow off of the 1-junction. The model of figure 3 includes a

modulated effort source that is used to model the hinge moment torque.

The fin dynamics model shows a nonlinear backlash element. The backlash model is expanded and shown in figure 4. As seen in figure 4, the gear positions on both sides of the backlash model are sensed. A specified amount of force is calculated and sent back through a modulated effort source depending on whether or not the gears are in contact. Although the bond-graph depicts the torque transmitted as an effort source, it is really modeled as a torsional spring, as follows:

if (*position error* > *backlash*/2) then
    Twist = (*position error* – *backlash*/2)
else if (*position error* < - *backlash*/2) then
    Twist = (*position error* + *backlash*/2)
else
    Twist = 0
end

The modulated effort source is then assigned a value of *k***Twist*, where *k* is a torsional spring constant that is set at a very stiff value (3000 in*Lbf/deg). This non-linearity causes problems in the position control of the fin.

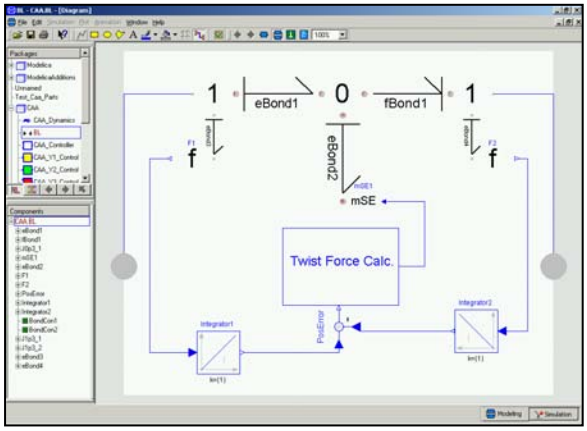

Figure 4. Backlash Model

Table 1 gives a list of values used in the actuator model.

Variable	Figure	Value	Variable	Figure	Value
e0	2A	130	jmotor	2B	5.00E-05
cbatt	2A	0.002	Rshaft	2B	2.5
Ibatt	2A	0.001	gk	3	0.6
battrsk	2A	2	acf	3	1
cdriver	2A	1.00E-05	FinFriction	3	0.4
Imotor	2B	6.00E-04	jacf	3	0.034
kmotor	2B	0.65	backlash	4	.05 (deg).

Table 1. Mode Parameter Values

Also, in figures 2 and 3 two integrators have been connected to two specific power bonds. In figure 2 the integrator is connected to the input power. This integrator calculates the total amount of energy supplied to the system. In figure 3 the integrator is connected to the bond between the 1-junction and the *I* element. This integrator calculates the total energy delivered to the fin.

CONTROLLERS

Two separate controllers are considered in this paper. The first controller is shown in figure 5. The fin

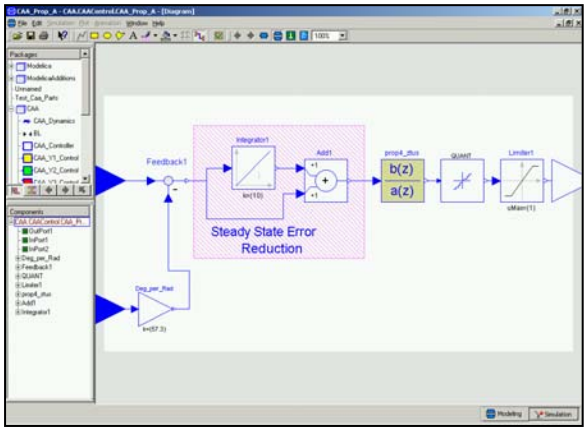

Figure 5. Controller 1

command is in degrees and the fin response enters the controller in radians. The steady-state error portion of the controller has a transfer function of 10/s + 1. The discrete transfer function, *prop4_ztus*, of figure 5 has the form shown in equation 1 with a sample rate of 6000 Hz.

$$G(Z) = \frac{(2.44E-4)*\left[Z^2 + 2Z + 1\right]}{Z^2 - 1.85 + 0.86} \qquad (1)$$

The quantizer relationship is shown in equation 2.

$$output = 0.015 * sign(input) * floor\left(\left|\frac{input}{0.015}\right|\right) \qquad (2)$$

The ± 1 limit is to keep the PWM output of the controller within the physical capabilities of the modulated transformer in figure 2.

Figure 6 shows the second controller that is considered in this paper. Similar to controller 1, controller 2 has a command input in degrees and a measured position input in radians. Also, the quantizer block and the ± 1 limit block are the same for the two controllers. Controller 2, however, is designed to operate at 1200 Hz. The delay on the output of controller 2

accounts for latency between the controller and the actuator.

As seen in figure 6, controller 2 has a distinctive anti-backlash element in the controller to counteract the backlash in the gear train. This backlash element adds a sign dependant bias to the control signal to push the gear train though the backlash region such that the gears stay in contact as much as possible. As expected, the backlash in the system causes a limit cycle in the steady-state response [3]. The anti-backlash element works to reduce the effects of the gear train backlash. The anti-backlash bias, denoted *Slide_Delta* in figure 6, is set at 0.028.

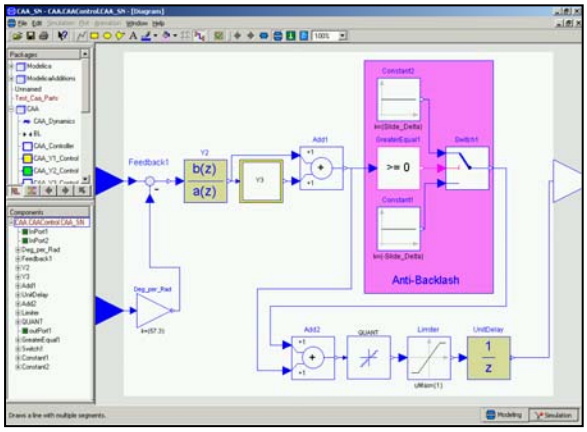

Figure 6. Controller 2

The transfer function for the element *Y2* is given by equation 3 with a sample rate of 1200 Hz.

$$Y2(Z) = \frac{0.172 * [Z - 0.688]}{Z - 0.453} \qquad (3)$$

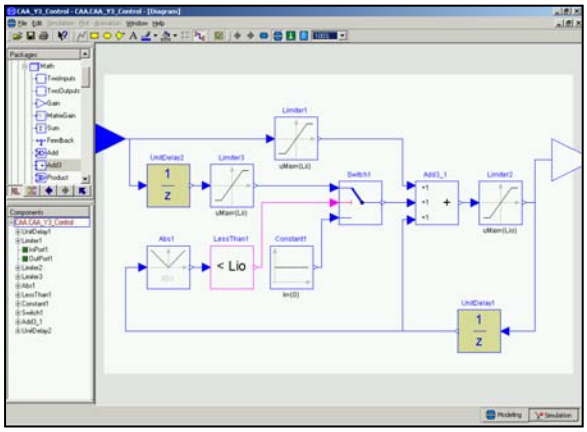

Figure 7. Content of the Y3 Element

The *Y3* element of figure 6 is expanded and shown in Figure 7. The *Y3* element serves as a non-linear limiter which, depending on the conditions shown in figure 7, moves a controller zero between 0 and -1 in the *Z*-plane, which adds conditional phase shift to the control signal. The value used for lii is 0.11, and the value of lio is 0.06.

Controller 1 is a much simpler scheme that does not actively try to cancel out the backlash of the system. The backlash will then add phase lag to the overall system. Controller 2 actively attempts to account for the backlash in the gear train. The anti-backlash in controller 2 then allows for a controller that can run at a slower rate without significant phase loss.

POWER FLOW CONSIDERATIONS

As can be seen in figures 1 and 2, no usable power comes from the controller. The controller simply signals the power flow in the actuator through the modulated transformer. This signal governs the amount of power flow throughout the entire system.

A comparison of the effectiveness of each of the two controllers can be made by observing their ability to utilize the power supplied by the motor. By monitoring the power flow through the bond-graph, one can get an idea of the effectiveness of any given controller. In order to monitor the power flow through the bond-graph, the bonds connected to sources and passive elements are special bonds that provide an additional power-signal output, as previously shown in figures 2 and 3.

The bond-graph of figure 2 shows that a power limit exists in the system. It is clear that the maximum power delivered to the fin cannot be more than exists in the power supply. In order to monitor the ability of the controller to utilize the power from the battery, an integrator has been connected to the power-bond of the input source in figure 2. This integrator measures the energy supplied to the system. Also, an integrator has been connected to the power-bond of the fin in figure 3. This integrator measures the amount of energy delivered to the fin. By dividing the output energy by the input energy, a control designer can get an idea of how efficient the controller is. This efficiency term introduced here is similar to the thermodynamic first law efficiency [4].

DYMOLA SIMULATION AND RESULTS

Figure 8 shows a step response for 10 degrees of commanded fin deflection. The hinge moment amount is set at -3 in*Lbf per degree of fin deflection. The solid line represents the fin response for controller 1. The dashed line represents the response for controller 2. The step command begins at .5 seconds to allow the integrators to initialize.

As can be seen in figure 8, controller 1 tries to zero out the steady-state error, which controller 2 is unable to do. A comparison to the thermodynamic theoretical limit is obtained by dividing the energy delivered to the fin by the energy input into the system. This normalization is

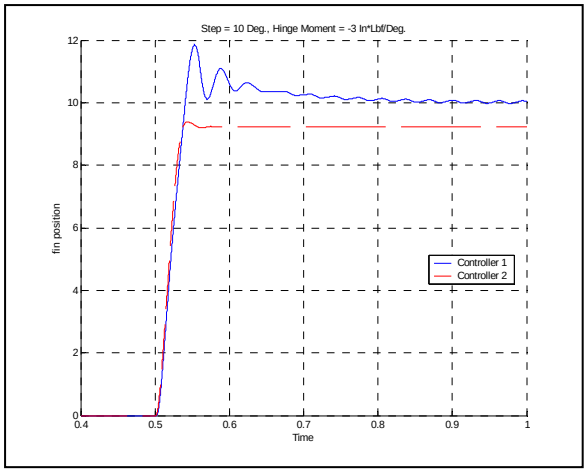

Figure 8. 10 Deg. Step, -3 In*Lbf/Deg Hinge Moment

shown in figure 9. The signals used for this evaluation come from the outputs of the extra integrators shown in figures 2 and 3. The plots for the two controllers in figure 9 are very similar. This calculation, however, still does not clarify, which of the two controllers is more efficient. In order to help clarify further, the signals of figure 9 are integrated and compared. These new signals are shown in figure 10. Since integration is a continuous summation, the integral of the signals in figure 9 *sums up* the normalized energy that is delivered to the fin.

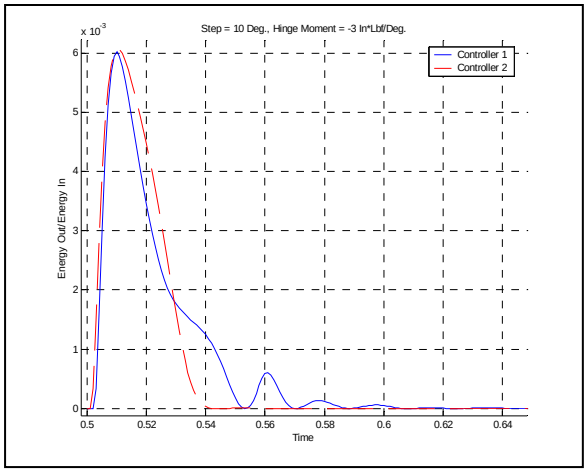

Figure 9. Energy Out/Energy In

By integrating the signals of figure 9 with respect to time, it is seen that initially, controller 2 supplies more energy to the fin. However the steady-state error reduction in controller 1 soon causes the energy response to catch up. These results are not surprising, since the step response in figure 8 shows that controller 2 is unable to zero out the steady-state error.

These results can be interpreted as controller 1 being more efficient, since more of the overall system's energy is being delivered to the fin.

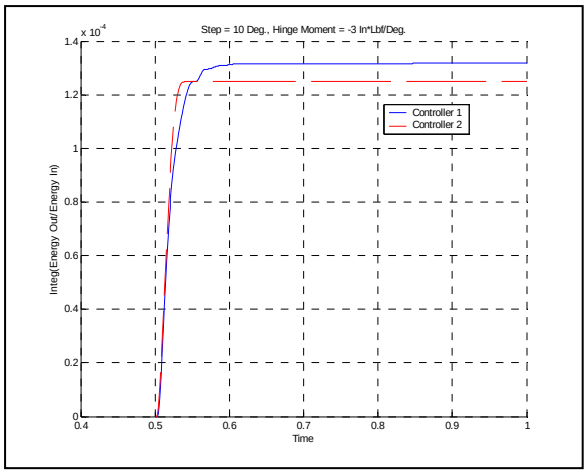

Figure 10. Integ (Energy Out/Energy In)

Figure 11 shows a step response for 3 degrees of commanded fin deflection. Again, the hinge moment amount is set at -3 in*Lbf per degree of fin deflection. The small step command generates a small hinge moment, since hinge moments are proportional to fin deflection.

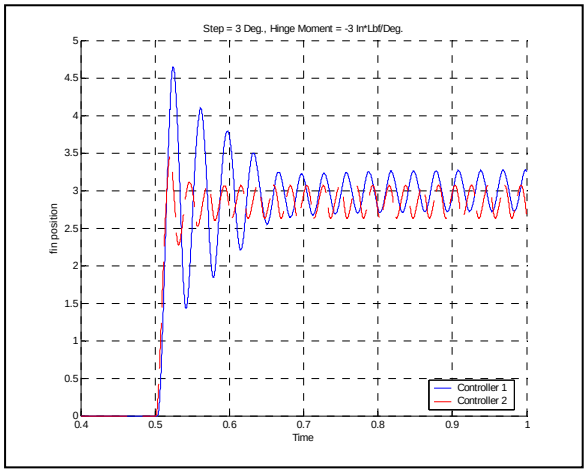

Figure 11. 3 Deg. Step, -3 In*Lbf/Deg Hinge Moment

The lack of hinge moment coupled with the backlash in the model has the effect of inducing a steady-state oscillation. As seen in figure 11, the amplitude of the steady-state oscillation is not as great for controller 2

when compared to controller 1. This is due to the non-linear anti-backlash element in controller 2

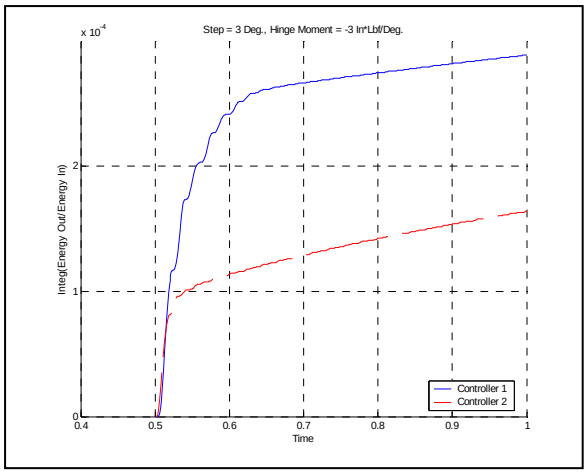

Figure 12. Integ (Energy Out/Energy In)

Similar to figure 10, figure 12 shows the integral with respect to time of the *Energy Out/Energy In* for the 3 degree step command. This comparison shows a dramatic difference between the effectiveness of controller 1 versus controller 2. The increased use of energy, as seen by the continued rising slopes in figure 12, comes from the steady-state oscillation of both controllers. The greater

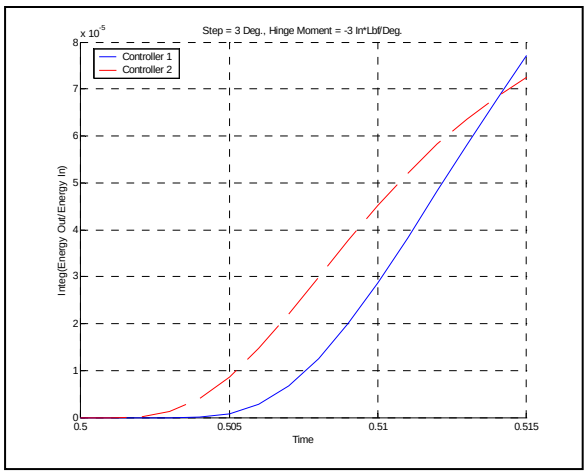

Figure 13. Integ (Energy Out/Energy In) *zoom*

effectiveness of controller 1 over controller 2 can even be seen prior to the establishment of the steady-state oscillation. Figure 13 shows this by zooming in on figure 12. Figure 13 shows that controller 2 does a better job of delivering energy to the fin initially, which gives a slightly quicker rise time.

Ideally, the steady-state slope of the signals in figure 12 would be zero since the desired output of the controller is a steady-state fin position from a step response input. However, given the fact that both controllers have difficulty with the backlash, low hinge moment induced, steady-state oscillation, a slope of zero is not possible for either controller. The controller must continually supply energy to the fin to fight the oscillation. The steady-state slope of controller 1, in figure 12, is less then the steady-state slope of controller 2. Eventually controller 2 will supply more energy to the fin to fight the steady-state oscillation than controller 1, making controller 2 more efficient in the presence of a steady-state oscillation. The anti-backlash element in controller 2 makes this possible.

Controller 1 is a more efficient controller in a large hinge moment environment, since it is able to zero out the steady-state error. Controller 2 however, is a more efficient controller in the presence of steady-state oscillation. Controller 2 runs at a slower rate than controller 1, and has a 1200 Hz delay between the generation of the control signal and the implementation of the control signal. Still, controller 2 does a better job of utilizing the energy in the system to fight the steady-state oscillation. This is also evident from the step responses shown in figure 11, since the response from controller 2 has a lower amplitude oscillation. The choice of selecting one controller over another, in this instance, then depends on the environment, in which the system is expected to be used.

As seen here, the two controllers produce stable results. This type of analysis, of course, should not be used in the presence of an unstable controller. Naturally, an unstable design will deliver a large amount of energy to the fin motion. Blindly maximizing the energy delivered to the fin, however, is not the goal. The goal is to maximize the energy output to the fin in a controlled manner. Ideally, we like to see a fast rise of the energy delivered to the actuator, followed quickly by a zero slope at high value, denoting that a stable stead-state value without oscillation has been reached.

In general, it is possible that one controller produces a steady-state oscillation, where another does not. In a linear system, this will occur if the overall closed-loop system has *s*-plane poles on the imaginary axis [5]. In this case, the controller with the steady-state oscillation will supply more energy to the fin than the controller that does not exhibit the oscillation. Thus, this analysis must be done with caution, in that the controllers being compared should produce similar responses.

CONCLUSIONS

This paper showed, by means of an example, a method in which the power flow obtained from a bond-

graph model can be used to compare the efficiency of controllers with different topologies. The actuator example used has two non-linear resistors and backlash in the gear train. One of the controllers shown, controller 2, uses a non-linear anti-backlash element in its control scheme to actively try and cancel the backlash in the gear train. Controller 1 however is a linear controller. Thus the two controllers presented here have very different topologies.

The normalization of the output energy to the input energy, from a bond-graph model of the actuator, allows the designer to compare the effectiveness of various controller schemes. The normalization of output energy to input energy gives a feel for how close the control scheme comes to the thermodynamic limit. This controller efficiency gives a method for comparing different control schemes, as long as all of the control schemes being compared are stable and produce similar step responses. No other restrictions are made. The analysis works for both linear and non-linear systems, and provides a good method for comparing controllers of each type.

Control engineers are frequently confronted with the problem of having to evaluate the quality of a particular design, made by one engineer, to others that were made by other engineers or even other companies. At the time of the comparison, the original design goals (performance indices in the optimization) may no longer be available, and it may thus be difficult to compare designs using completely different controller structures to each other.

The qualitative, energy-based control evaluation method introduced in this paper offers a cheap and convenient means to do so.

Bond-graph modeling lends itself naturally to this type of analysis, since it maps the power flow through the system. Once the power flow map, from a bond-graph of the controller's actuation system, has been established, it is a relatively simple task to monitor the energies delivered to the various branches of the system.

REFERENCES

[1] DYMOLA Dynamic Modeling Laboratory, World Wide Web page http://www.Dynasim.se.

[2] Cellier, F.E., and R.T. McBride (2003), "Object-Oriented Modeling of Complex Physical Systems Using the Dymola Bond-Graph Library," *Proc. ICBGM'03 Conference*, Orlando, Florida.

[3] Marquez, H. (2003), "Nonlinear Control Systems, Analysis and Design", *John Wiley & Sons*

[4] Cengel, and Boles (1989), "Thermodynamics: An Engineering Approach" p. 293, *McGraw Hill*

[5] Kailath, T. (1980), "Linear Systems", *Prentice Hall*